Cerebral Cortex January 2010;20:214–228
doi:10.1093/cercor/bhp091
Advance Access publication May 22, 2009

Cerebellar Inputs to Intraparietal Cortex Areas LIP and MIP: Functional Frameworks for Adaptive Control of Eye Movements, Reaching, and Arm/Eye/Head Movement Coordination

Vincent Prevosto[1], Werner Graf[2] and Gabriella Ugolini[1]

[1]Laboratoire de Neurobiologie Cellulaire et Moléculaire (NBCM), UPR9040 CNRS, 91198 Gif sur Yvette, France and [2]Department Physiology and Biophysics, Howard University College of Medicine, Washington, DC 20059, USA

Using retrograde transneuronal transfer of rabies virus in combination with a conventional tracer (cholera toxin B), we studied simultaneously direct (thalamocortical) and polysynaptic inputs to the ventral lateral intraparietal area (LIPv) and the medial intraparietal area (MIP) in nonhuman primates. We found that these areas receive major disynaptic inputs from specific portions of the cerebellar nuclei, the ventral dentate (D), and ventrolateral interpositus posterior (IP). Area LIPv receives inputs from oculomotor domains of the caudal D and IP. Area MIP is the target of projections from the ventral D (mainly middle third), and gaze- and arm-related domains of IP involved in reaching and arm/eye/head coordination. We also showed that cerebellar cortical "output channels" to MIP predominantly stem from posterior cerebellar areas (paramedian lobe/Crus II posterior, dorsal paraflocculus) that have the required connectivity for adaptive control of visual and proprioceptive guidance of reaching, arm/eye/head coordination, and prism adaptation. These findings provide important insight about the interplay between the posterior parietal cortex and the cerebellum regarding visuospatial adaptation mechanisms and visual and proprioceptive guidance of movement. They also have potential implications for clinical approaches to optic ataxia and neglect rehabilitation.

Keywords: forward models, optic ataxia, prism adaptation, rabies, transneuronal

Introduction

To generate goal-directed movements, such as reaching with the arm at stationary or moving objects, the brain must specify the position of the target in an egocentric frame of reference by integrating external signals (e.g., visual and auditory) relative to target position with intrinsic congruent signals (proprioceptive, vestibular, motor) related to body, arm, head, and eye positions. The posterior parietal cortex (PPC), which is part of the visual dorsal stream and is reciprocally connected with motor areas of the frontal lobe, is an important sensorimotor interface for intentional and attentional planning and online control of sensory guided, goal-directed, movements (Colby and Goldberg 1999; Buneo and Andersen 2006; Mulliken et al. 2008).

To circumvent sensory feedback delays, current motor control theories postulate the existence of "forward" models, combining sensory inputs with motor commands to maintain a continuous estimate of movement state. According to recent hypotheses, both the PPC and the cerebellum would be part of forward models (Desmurget and Grafton 2000; Blakemore and Sirigu 2003; Buneo and Andersen 2006; Mulliken et al. 2008). Their reciprocal connectivity (Sasaki et al. 1977; Stein and Glickstein 1992; Kakei et al. 1995; Clower et al. 2001, 2005) makes it likely that they form functional loops for rapid predictions of the sensory consequences of action and online updating of movement plans.

The cerebellum influences the PPC via cerebellothalamocortical pathways (Kakei et al. 1995). However, the presence of cerebellar terminations (Kalil 1981; Asanuma et al. 1983; Stanton and Orr 1985) in thalamic nuclei that project to the PPC (e.g., Asanuma et al. 1985; Schmahmann and Pandya 1990; Hardy and Lynch 1992; Amino et al. 2001) could not clarify precisely the origin and extent of cerebellar inputs to individual PPC areas due to the overlap of different thalamocortical populations in the same thalamic domains.

A major advance has been the development of retrograde transneuronal tracers, which makes it possible to map cerebellar input to individual cortical areas with great precision. With regard to the PPC, it has been shown that among areas 7a, 7b, the dorsal portion of the lateral intraparietal (LIPd) area, and the anterior intraparietal (AIP) area, only areas 7b and AIP receive cerebellar inputs (Clower et al. 2001, 2005).

Using retrograde transneuronal transfer of rabies virus (Ugolini 1995, 2008; Ugolini, Klam, et al. 2006), we clarified here in nonhuman primates the origin of cerebellar inputs to 2 further PPC areas, that is, the ventral lateral intraparietal area (LIPv) and the medial intraparietal area (MIP) in the lateral and medial bank of the intraparietal sulcus (IPS), respectively. Injections were targeted into rostral LIPv and MIP at the middle third level of the rostrocaudal extent of the IPS (Fig. 1).

LIPv is an eye movement area distinct from LIPd in myelo- and cytoarchitecture, visual field representation, and connectivity (Blatt et al. 1990; Lewis and Van Essen 2000). The ensemble of LIPd and LIPv is regarded as the "parietal eye field," as it contains an eye-centered representation of the space explored by eye movements, it is involved in shifting visuospatial attention and participates in encoding saccades toward salient teleceptive cues (Colby and Goldberg 1999; Buneo and Andersen 2006).

The targeted portion of MIP (Fig. 1) is the rostral end of MIP as cytoarchitectonically defined by Colby et al. (Colby et al. 1988) that according to other nomenclatures, corresponds to the middle third of PEa (Seltzer and Pandya 1986; Battaglia-Mayer et al. 2006) or PEip (Matelli et al. 1998), PA5 (Kalaska and Crammond 1992), 5b (Bioulac et al. 1999), or 5V (Lewis and Van Essen 2000). Like the more caudally located parietal reach region (Buneo and Andersen 2006), this portion of MIP is an arm movement–related area, involved in sensory guidance of reaching (Mountcastle et al. 1975; Burbaud et al. 1991; Kalaska and Crammond 1992; Iriki et al. 1996; Johnson et al. 1996). It contains neurons responsive to somatosensory (especially arm proprioceptive) and visual signals (Mountcastle et al. 1975; Seal et al. 1982; Burbaud et al. 1991; Colby and Duhamel 1991) as well as vestibular signals evoked by self-motion that also

© The Author 2009. Published by Oxford University Press. All rights reserved.
For permissions, please e-mail: journals.permissions@oxfordjournals.org

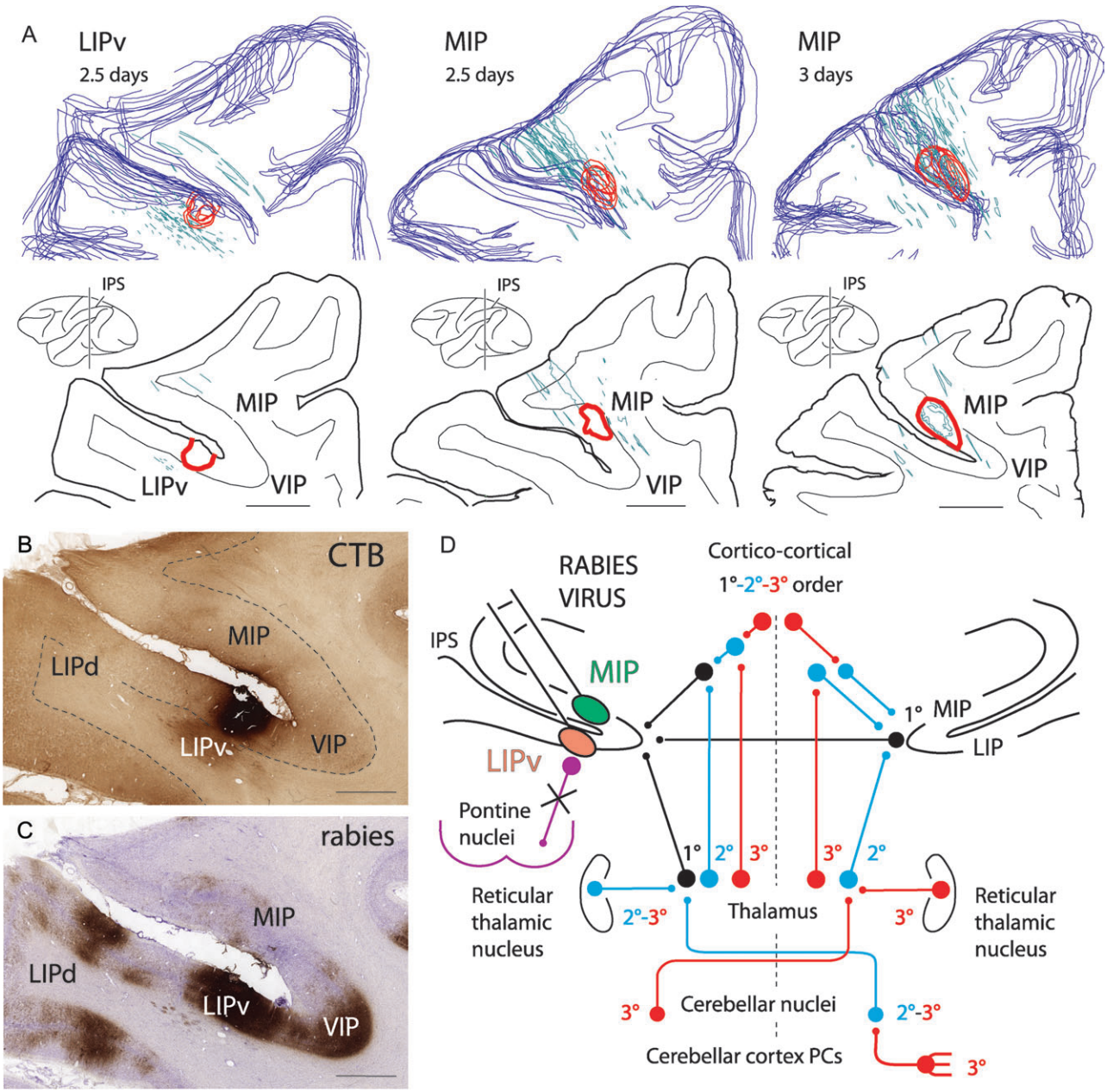

Figure 1. (*A*) 3D reconstructions and coronal sections of the injection area (red outlines) into the LIPv or the MIP at the level of the middle rostrocaudal third of the IPS, visualized by CTB immunolabeling at 2.5 or 3 days after injection of a mixture of rabies and CTB. Blue outlines: cortical surface. Green outlines: reconstructions of electrode tracts from previous recordings. (*B, C*) Photomicrographs of adjoining sections at the LIPv injection site, immunolabeled for CTB and rabies virus (same level as in A, left). Note that the injection area is easily identifiable with CTB (*B*) but not with rabies virus (*C*) at 2.5 days because of strong rabies immunolabeling of short-distance projections neurons in the IPS. In (*B*), shading in the white matter ventral to LIPv is background staining of an area of fibrosis due to multiple recording traces in that region. (*D*) Summary of the pathways of rabies retrograde transneuronal transfer to the cerebellar nuclei after coinjection of rabies virus and CTB into ventral MIP or LIPv: 1° (black), first-order neurons (conventional tracer, CTB) in the ipsilateral thalamus and cortical areas (ipsilateral corticocortical inputs, callosal inputs from homotopic IPS areas); 2° (blue), second-order neurons labeled transneuronally (rabies virus) at 2.5 days in the contralateral cerebellar nuclei, in the ipsilateral thalamic nuclei and reticular thalamic nucleus, and in the contralateral thalamic nuclei (the latter reflecting projections to IPS areas of the right hemisphere); 3° (red), third-order neurons labeled at 3 days in the contralateral cerebellar cortex (PCs) and contralateral reticular thalamic nucleus. Anterograde transneuronal transfer (e.g., to the pontine nuclei) did not occur (violet). Scale bar = 4000 μm in (*A*), 2000 μm in (*B*) (also applies to *C*).

discriminate active from passive movement (Klam and Graf 2003, 2006) and bimodal neurons with congruent visual-somatosensory receptive fields that are dynamically modified by tool use (Iriki et al. 1996). Activity in this rostral portion of MIP during arm movement preparation and execution is influenced by motivation and is highly tuned to movement direction and kinematics but not dynamics (Mountcastle et al. 1975; Seal et al. 1982; Crammond and Kalaska 1989; Johnson et al. 1996; Hamel-Pâquet et al. 2006). Early neuronal discharge in MIP overlaps M1 activity and movement onset, and late neuronal discharge is strongly influenced by arm proprioceptive inputs (Burbaud et al. 1991; Bioulac et al. 1999).

By coinjecting rabies virus and a conventional tracer into LIPv or MIP, we were able to visualize simultaneously thalamocortical

and other direct projections to these areas (conventional tracer) and higher order inputs (rabies virus). We found that LIPv and MIP receive major disynaptic projections from specific portions of the cerebellar nuclei. We also clarified the origin of trisynaptic projections to MIP from specific cortical cerebellar populations. Preliminary accounts of our findings have been reported earlier in short form (Ugolini et al. 2005; Ugolini, Prevosto, et al. 2006, 2007).

Materials and Methods

Rabies transneuronal tracing experiments were carried out in 3 adult macaque monkeys (1 *Macaca fascicularis*, 2 *Macaca mulatta*). Animals were purpose bred and purchased from authorized suppliers. Animal care and experimental procedures were approved by the relevant institutional bioethical committees and conformed with national laws and the European Communities Council Directive of 24 November 1986 (86/609/EEC) concerning biosafety and use of laboratory animals in research, as well as with "Principles of Laboratory Animal Care" (National Institutes of Health publication No. 86-23, revised 1985). Details on preparation of rabies virus, handling of virus-infected animals, and the methodology for transneuronal tracing using rabies virus were described previously (Ugolini 1995, 2008; Ugolini, Klam, et al. 2006).

MIP and LIPv Injection Sites: Neuronal Properties

Injections into ventral MIP (2 monkeys) and LIPv (1 monkey) were made at the end of long-term electrophysiological recordings. Neurons at the MIP injection site were characterized by prominent vestibular responses (Klam and Graf 2003, 2006), as well as somatosensory and bimodal somatosensory/visual responses (see also Colby and Duhamel 1991; Iriki et al. 1996). Directional visual tuning was less selective than that of neurons in the ventral intraparietal (VIP) area, and somatosensory receptive fields were located on the arms and hands (Klam and Graf 2003), as characteristic of MIP, but not the face, as found in VIP (Colby and Duhamel 1991; Bremmer et al. 2002). Neurons at the LIPv injection site had visual and eye movement–related responses characteristic of LIPv (Blatt et al. 1990, Ben Hamed et al. 2001), weak vestibular responses, and no somatosensory responses characteristic of VIP (e.g., Colby and Duhamel 1991).

Surgical Procedures, Injections, and Postoperative Care

Surgery was performed aseptically under general anesthesia. After premedication with Valium (10 mg) and atropine (0.5 mg) and induction of anesthesia with Ketamine (30 mg/kg intramuscular [im]) and acepromazine (0.5 mg/kg im), venous access was established, and the intravenous anesthetic propofol (induction dose, 10 mg/kg; maintenance dose, 15 mg/kg/h) was administered during the procedure. The monkey's head was fixed in a stereotaxic head holder. Access to ventral MIP or LIPv was gained via the previously implanted recording chamber, which was equipped with a Teflon grid for electrode placement, thereby allowing highly reproducible electrode penetrations. Injections were targeted at stereotaxic coordinates of previously recorded responses (Klam and Graf 2006) (see above). A mixture of rabies virus solution (Challenge Virus Standard [CVS] strain, 5.96×10^{10} PFU/mL) and cholera toxin B fragment (CTB) (low salt, end concentration 0.03%) (List Biological Labs, Campbell, CA) (Luppi et al. 1990) was injected in a single dose (2 μL delivered over 30 min) into the ventral MIP (2 monkeys) or LIPv (1 monkey) at midpoint of the rostrocaudal length of the IPS of the left hemisphere via a Hamilton syringe driven by a micromanipulator. The injection needle was left in place for more than 30 min after the end of the injection. After recovery from general anesthesia, the animals behaved normally without any clinical or behavioral signs of infection (Ugolini, Klam, et al. 2006).

Time Points of Transfer

Animals were euthanized for histological examination 2.5 days (experiments MIP-2 and LIPv-1) and 3 days (MIP-1) after injection. These time points are sufficient for rabies retrograde transneuronal labeling of second-order neurons (2.5 days) and third-order neurons (3 days) (Moschovakis et al. 2004; Ugolini, Klam, et al. 2006) and simultaneous retrograde labeling of first-order neurons (CTB).

Perfusion, Tissue Processing, and Immunohistochemistry

At the chosen time points, the animals were given a lethal dose of pentobarbital (30 mg/kg intravenous) after induction of deep general anesthesia as described above. They were perfused transcardially with 2 L of phosphate-buffered saline (pH 7.4), followed by 3.5 L of 4% paraformaldehyde in 0.1 M phosphate buffer (PB) (pH 7.4) and 4 L of 10% sucrose in 0.1 M PB (pH 7.4). Brains were cut stereotaxically in the frontal plane in 2 blocks, cryoprotected and gelatin embedded as described previously (Ugolini, Klam, et al. 2006), and cut in frozen serial sections (50 μ), which were collected free floating in 8 parallel series. In 2 series (200-μm spacing), rabies virus was visualized immunohistochemically using a monoclonal antibody directed against the rabies P protein (diluted 1:1000) and the peroxidase–antiperoxidase method as described previously (Ugolini, Klam, et al. 2006). After reactions, sections were mounted on gelatin-coated slides, air dried, counterstained with 0.1–0.5% Cresylviolet (Sigma-Aldrich, Lyon, France), and coverslipped with Entellan (Merck, Whitehouse Station, NJ). In an adjoining series of sections, CTB labeling was visualized using the peroxidase–antiperoxidase method. Sections were incubated at room temperature in triton 0.4% for 30 min, 10% donkey serum for 1 h, followed by 8-day incubation at 4 °C with goat anti-choleragenoid (List Biological Labs) (1:5.000), 2-h incubation at room temperature in donkey anti-goat IgG (Jackson ImmunoResearch Labs, West Grove, PA) (1:200) and 2 h in goat peroxidase–antiperoxidase complex (Jackson ImmunoResearch Labs) (1:400), followed by detection of peroxidase activity by 30-min incubation in a metal-enhanced diaminobenzidine substrate kit (Pierce, Rockford, IL). Sections were mounted on gelatin-coated slides, air dried, and coverslipped with Entellan (Merck). Another series of sections was stained for myelin with gold chloride (Schmued 1990).

Data Analysis

We examined every fourth section for rabies immunolabeling and every eighth sections for CTB immunolabeling. Labeled neurons were visualized by light microscopy, analyzed, and counted using a computer-assisted plotting and reconstruction software (Neurolucida, MBF Bioscience, Colchester, VT). 3D reconstructions of the injection area, the cerebellar nuclei, and the entire cerebellar cortex were created using Neurolucida, by stacking in register serial digital plots of immunolabeled sections. Solid reconstructions were visualized using the associated Solid Model software and exported into Adobe Illustrator. High-resolution composites of digital images were captured using an Optronics video camera coupled to the microscope and the Virtual Slice module of Neurolucida.

Results

In these experiments, we found that it is possible to coinject a mixture of rabies virus and the conventional tracer CTB without altering the uptake of either tracer (see below). This is a major methodological improvement because it allows visualization in the same experiment of the injection area and of direct projections (here thalamocortical and other first-order neurons) with CTB, as well as transneuronal labeling (higher order neurons) with rabies virus. This rabies–CTB combination has also the great value of avoiding any difficulties in interpretation that would arise in case of slightly different placement of the injections if single-step and transneuronal tracing experiments were conducted separately (with the bonus that the number of nonhuman primates required to obtain the 2 sets of results is reduced by half).

Injection Site (CTB Results)

Contrary to some conventional tracers and alpha-herpesviruses (e.g., Hoover and Strick 1999), rabies virus does not induce tissue damage and does not accumulate at the injection site. Therefore, the injection site can only be estimated based on the density gradient of labeled neurons (Kelly and Strick 2003) that can be complicated by labeling of short-distance projection neurons (Fig. 1*C*). Conversely, after coinjection of rabies virus and CTB, CTB immunolabeling reveals the precise extent of the injection site, which is a major improvement (Fig. 1*B*) (Ugolini et al. 2005; Billig and Strick 2006). Reconstructions of the injection sites (Fig. 1*A*) and study of the myelo- and cytoarchitectonics showed that the injections involved area LIPv (see Blatt et al. 1990; Lewis and Van Essen 2000) or the ventral portion of MIP at the level of the middle rostrocaudal third of the IPS (Fig. 1; see the introduction for correspondence with other nomenclature). The injections did not invade either the white matter or area VIP (Fig. 1), in keeping with neuronal responses at the injection sites (see Materials and Methods).

First-Order Inputs (CTB Results): Differences in Thalamic Input to MIP and LIPv

Because we deliberately used CTB at low concentration (0.03%) in order not to interfere with rabies virus uptake, CTB immunolabeling was not very intense but easily detectable. Importantly, CTB immunolabeling visualized all known direct thalamocortical and corticocortical projections to MIP and LIPv (e.g., frontoparietal, Graf et al. 2006), showing that mixing rabies with CTB did not alter CTB uptake. The thalamic nuclei were delineated according to Olszewski (Olszewski 1952) (Fig. 2). CTB results showed that the first-order thalamic neurons targeting LIPv and ventral MIP were largely topographically segregated (Fig. 2, white dots). Thalamic input to MIP was derived ipsilaterally from mainly dorsal and lateral portions of the lateral pulvinar (LPul), anterior pulvinar (APul), lateralis posterior (LP), ventral lateral, pars postrema (VLps) and pars caudalis (VLc), and neighboring central lateral (CL) and medial dorsal (MD) nuclei (Fig. 2). Thalamic input to LIPv originated largely from more caudal, medial, and ventral portions of the pulvinar complex (medial pulvinar, MPul, LPul, APul) and the LP, MD, and CL nuclei. Direct cortical projections to each area were derived from homotopic portions of the IPS of the contralateral hemisphere (Fig. 1*D*) and additional cortical areas of the ipsilateral hemisphere, including strong projections to MIP from area V6A (not shown) (for frontoparietal inputs, see Graf et al. 2006).

Rabies Transneuronal Transfer: Disynaptic Inputs (2.5 days) and Trisynaptic Inputs (3 days)

In these experiments, we found that mixing rabies virus with 0.03% CTB did not reduce transneuronal transfer of rabies virus, as confirmed by other authors (Billig and Strick 2006) who tested our rabies–CTB combination protocol in rodents. In fact, retrograde transneuronal transfer of rabies virus remained strictly time dependent: second-order and third-order neurons were labeled at 2.5 and 3 days, respectively (see below), as obtained in primates when we injected rabies virus alone (e.g., Moschovakis et al. 2004; Ugolini, Klam, et al. 2006; Ugolini 2008). No rabies immunolabeling was found in parietal receiving portions of the striatum, pontine nuclei, and nucleus reticularis tegmenti pontis (NRTP) at 2.5 or 3 days, confirming that rabies virus does not propagate by anterograde transneuronal transfer (e.g., Kelly and Strick 2003; Ugolini 2008).

Thalamus

Thalamic neuronal labeling provides an internal control of the number of synapses crossed by the rabies tracer. Apart from first-order, only disynaptic (second-order) projections were labeled at 2.5 days because labeling of the reticular thalamic nucleus was present ipsilaterally (i.e., second-order), but not contralaterally (third-order) (Fig. 2). Second-order neurons were labeled in additional thalamic nuclei on both sides (Fig. 2). Notably, at 2.5 days, second-order labeling in the contralateral (right) thalamus occurred in both MIP and LIPv experiments (LIPv: arrows in Fig. 2) and mirrored the distribution of first-order labeling (CTB) ipsilaterally because it reflected thalamocortical projections to homotopic IPS areas of the right hemisphere (which are first-order to the injected left MIP and LIPv, see Fig. 1*D*). At 3 days (experiment MIP-1), the rabies tracer crossed an additional synaptic step, as signaled by the labeling of the contralateral reticular thalamic nucleus, as well as additional thalamic domains (Fig. 1*D*).

Cerebellar Nuclei

At the 2.5 days time point, we also found second-order labeling in the cerebellar nuclei, showing that the intraparietal cortex receives prominent disynaptic cerebellothalamocortical projections (Fig. 1*D* and 3–6). At this time point, no labeling occurred in the cerebellar cortex (third-order) in the MIP and LIPv experiments. These results revealed important differences in cerebellar nuclear projections to ventral MIP versus LIPv.

Second-order cerebellar nuclear input to MIP was derived mostly from 2 regions in contralateral cerebellum (Figs 3 and 4). One was the ventrolateral part of the interpositus posterior (IP) nucleus, especially caudally (Fig. 3, left; Figs 4, 5*A-C*, and 6). The second region was the ventral portion of the caudal two-thirds of the contralateral dentate (D) nucleus, especially its middle third (Fig. 3, left; Figs 4, 5*G*, and 6). Only a few inputs were derived from the fastigial (F) nucleus bilaterally and from the interpositus anterior (IA) nucleus contralaterally, especially rostrally (Fig. 3, left; Figs 4 and 6).

By contrast, cerebellar input to LIPv was derived largely from different output channels (Fig. 3, right; Fig. 4; Fig. 5*D-F,H*; Fig. 6). Thus, the ventrolateral IP also targeted LIPv, but labeled neurons were fewer and occupied a more restricted portion of the ventrolateral IP contralaterally; most labeling of the D was located more caudally (Fig. 3, right; Fig. 4; Fig. 5*D-F,H*; Fig. 6). Only a few inputs were derived from the contralateral IA (caudal half); labeling of the F was negligible (Fig. 3, right; Figs 4 and 6).

At 3 days (third-order time point, MIP-1 experiment), the focus of the distribution in the cerebellar nuclei remained contralaterally in the same portions of ventral D and ventrolateral IP as obtained at the 2.5-day time point, but labeling extended to additional portions of all cerebellar nuclei bilaterally (Ugolini et al. 2005). This additional labeling is compatible with cerebellar nuclear projections to cortical areas connected to MIP, like third-order thalamic labeling (Fig. 1*D*). Thus, ipsilateral cerebellar labeling at 3 days mirrored the distribution obtained contralaterally at 2.5 days and most likely reflected projections to the right MIP (connected with the injected left MIP, Fig. 1*D*).

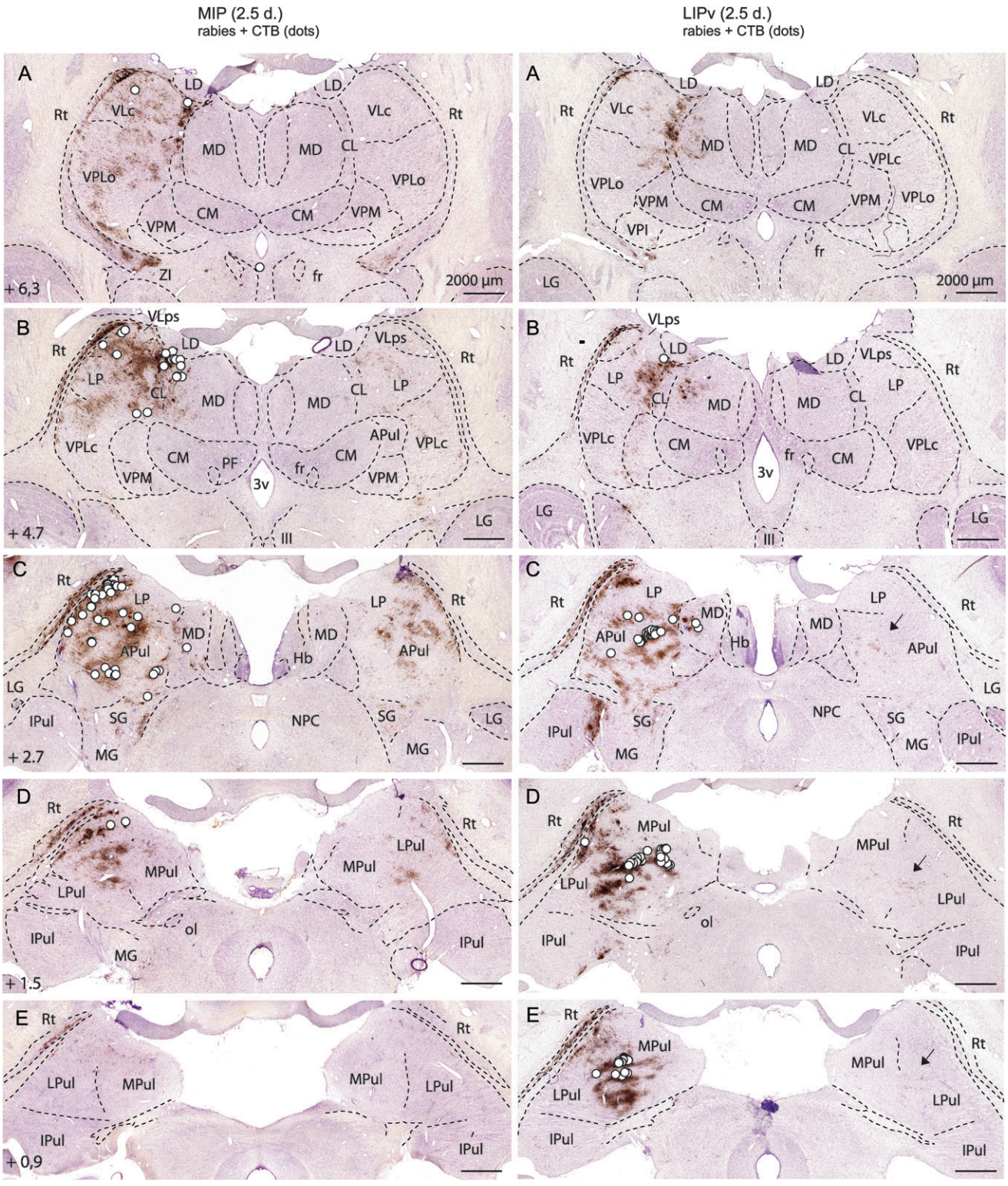

Figure 2. Differences in thalamic (direct and second-order) inputs to the MIP (left) versus the LIPv (right) at 2.5 days after coinjection of rabies virus and the conventional tracer CTB. In each row, the left side is ipsilateral. The rostrocaudal distance of the coronal sections from the interaural axis is indicated. White dots: first-order neurons (CTB); note the topographical differences of neurons targeting MIP (dorsal and lateral) versus LIPv (caudal, medial, and ventral). Location: pulvinar complex, LP, VLps and VLc, CL, MD. Brown: rabies retrograde transneuronal labeling at 2.5 days, involving second-order neurons in the reticular thalamic (Rt) nucleus ipsilaterally and additional thalamic nuclei on both sides. Second-order neurons (brown) contralaterally (for LIPv, see arrows in *C–E*) mirror the distribution of first-order neurons (white dots) ipsilaterally. In both MIP and LIPv experiments, no labeling is found in Rt (third order) contralaterally, showing that third-order neurons are not yet labeled at 2.5 days (see also Fig. 1*D*). Other abbreviations: CM, centromedian; fr, fasciculus retroflexus; Hb, habenula; IPul, inferior pulvinar; LD, lateral dorsal; LG, lateral geniculate; MG, medial geniculate; MPul, medial pulvinar; NPC, nucleus of the posterior commissure; ol, olivary pretectal nucleus; PF, parafascicular; SG, suprageniculate; VPLc, ventral posterior lateral, pars caudalis; VPLo, ventral posterior lateral, pars oralis; VPM, ventral posterior medial; ZI, zona incerta; 3v, third ventricle; III, oculomotor nucleus.

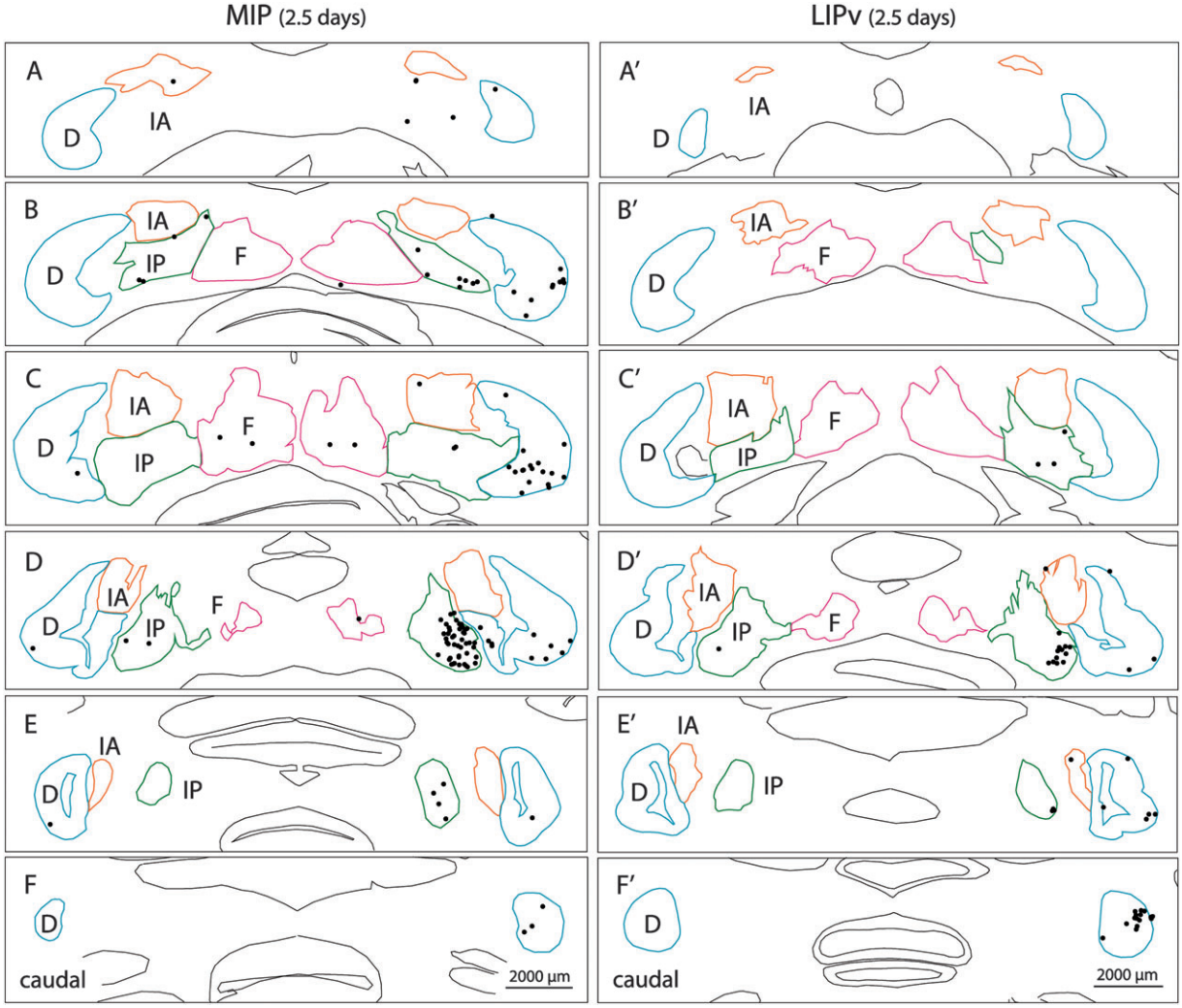

Figure 3. Differences in second-order inputs from the cerebellar nuclei to the MIP versus the LIPv (2.5 days). Projections to MIP are derived, mostly contralaterally, from the ventrolateral part of the IP and from mainly ventral domains of the caudal two-thirds of the D, especially middle third. Fewer inputs originate from the IA (especially rostral half) and the F nuclei. By contrast, inputs to LIPv are derived from a more restricted portion of ventrolateral IP and from the caudal pole of the D. In the IA, neurons targeting LIPv are caudal to those targeting MIP; labeling of F is negligible. Cross sections are arranged rostrocaudally from A to F (levels indicated in Fig. 4). Cerebellar nuclei are color coded (blue: D; green: IP; orange-brown: IA; magenta: F).

Third-Order Inputs to MIP from the Cerebellar Cortex

Results obtained at 3 days after injections into MIP revealed the topographic arrangements of cerebellar Purkinje cells (PCs) that influence trisynaptically MIP (via projections to cerebellar nuclei neurons labeled at 2.5 days) (Figs 1*D*, 5*I-M*, 7, and 8). The cerebellar cortical lobules (Figs 7 and 8) were identified according to Madigan and Carpenter (Madigan and Carpenter 1971). The majority (88%) of the labeled PCs was located in 5 regions of the contralateral cerebellar cortex (Fig. 7, pie chart), which can be grouped into 3 main groups.

The most prominent group (50.6%) included deep portions of Crus II posterior (Crus IIp, 30.9%) and the neighboring paramedian lobule (PML, 19.7%), where labeled PCs were arranged in multiple parallel bands, extending obliquely (from caudomedial to rostrolateral) with continuity across both Crus IIp and PML (Fig. 7*a-e*; Fig. 8*a,a',b,b',d,d'*; Fig. 5*I-M*). The densest (central) strip in PML/Crus IIp presumably corresponded in location to the olivocerebellar C2 zone, which receives input from the rostral medial accessory olive (rMAO) and projects to the IP, as described in other species (Rosina and Provini 1983; Voogd et al. 2003). A more lateral strip, particularly developed in Crus IIp, presumably corresponded in location to the D zones, projecting to the D nucleus (Rosina and Provini 1983; Voogd et al. 2003).

The second main group (26.1%) included paravermal portions of the anterior lobe (AL) (15.4%) and lobulus simplex (10.7%), where labeled PCs were aligned longitudinally in multiple bands of varying density, mainly on the dorsal paravermal surface of lobules V–VI (Fig. 7*e-j*, pie chart; Fig. 8*a, a', c, c', e, e'*).

The third main group included the dorsal paraflocculus (DPFl, 11.6%), where labeled PCs formed complex bands, located especially in the lateral half of the DPFl lobules, excluding the lobus petrosus (Fig. 7h-j; Fig. 8*a,a',b,b'*). The remainder (11.7%) was sparsely distributed in Crus Ip and Ia, vermal portions of AL, vermal VIII, IX–X, flocculus, and ventral paraflocculus (Figs 7 and 8). No labeling occurred in the oculomotor vermis (VII). Labeled PCs were clearly third-order neurons because granule cells

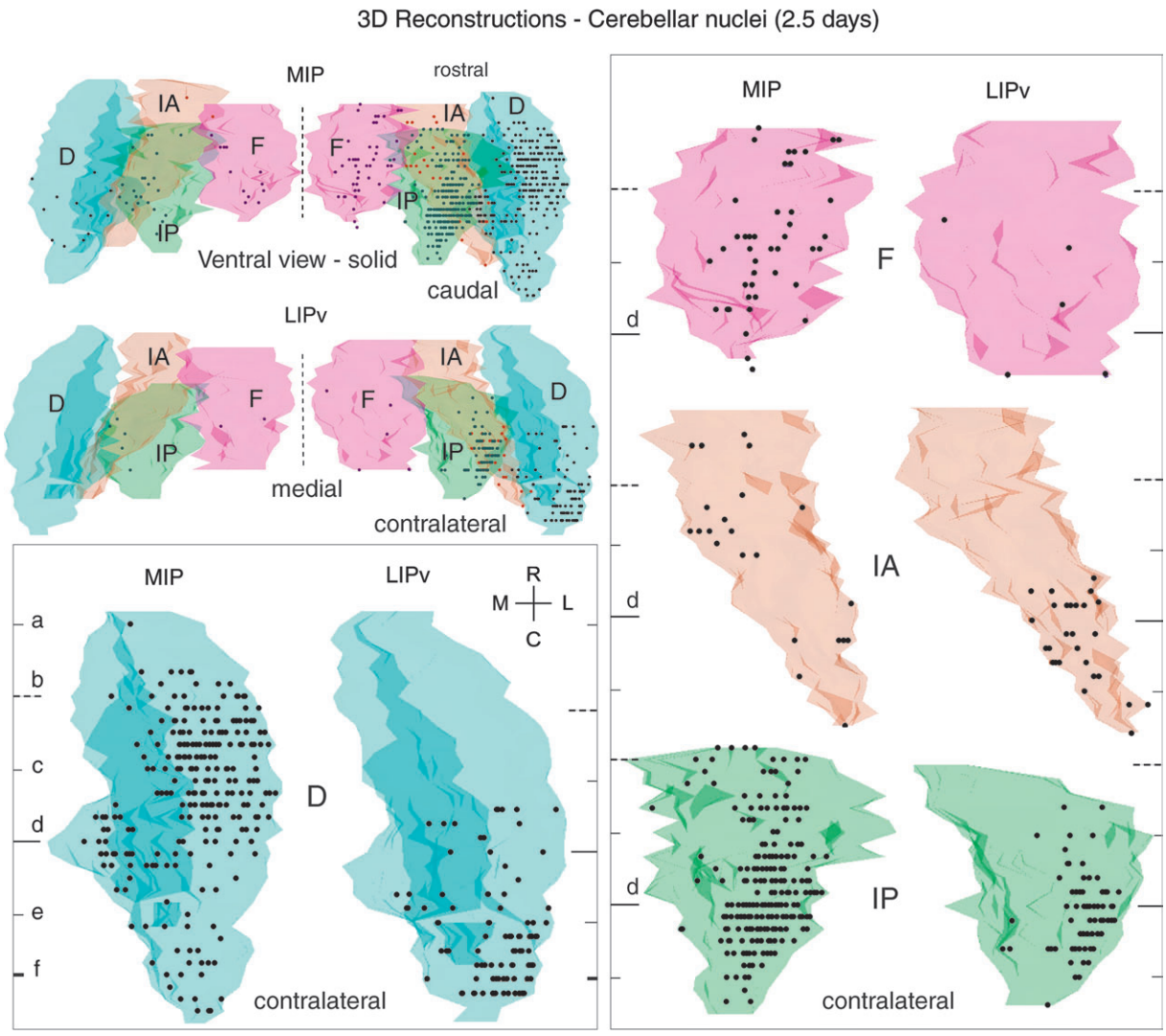

Figure 4. 3D reconstructions of the cerebellar nuclei, showing differences in second-order cerebellar nuclear inputs to the MIP versus the LIPv at 2.5 days (disynaptic inputs via cerebellothalamocortical projections). The 3D reconstructions were made using Neurolucida by stacking together serial 50-μm sections (200-μm spacing). Ventral views (−90° rotation from the plane of the cross sections in Fig. 3, viewed using Solid Model) are shown here in solid mode, without perspective, for the ensemble of the cerebellar nuclei (top left) and for individual contralateral nuclei (boxed images). In this figure and Figure 8, ventral views have been flipped on the *y*-axis to show the contralateral (right) cerebellum on the right side. In boxed images, horizontal lines indicate the levels of the cross sections shown in Figure 3 (same letter index). Cerebellar nuclei are color coded as in Figure 3 (blue: D; green: IP; orange-brown: IA; magenta: F). Note the predominantly contralateral distribution of transneuronally labeled neurons (dots), with major input to both MIP and LIPv from IP and D and minor contributions from IA and F, and the prominent topographical differences of the cerebellar populations targeting MIP versus LIPv.

(Kelly and Strick 2003) and cerebellar cortical interneurons (fourth order) were not yet labeled.

Discussion

Using retrograde transneuronal tracing with rabies virus, we found that the PPC areas LIPv and MIP (Fig. 1) receive prominent projections from the D and IP nuclei. The major IP output channels to these areas are in marked contrast with the minor inputs from the interpositus complex to the other parietal and frontal cortical areas studied to date that receive mostly D output channels (e.g., Dum and Strick 2003; Akkal et al. 2007).

Cerebellar projections are routed to the PPC through the dorsal thalamus. By injecting a mixture of rabies virus and a conventional tracer (CTB), we were able to identify direct projections to LIPv and MIP (CTB) and higher order neurons (rabies virus) in the same experiments. The CTB results showed that thalamocortical projections to LIPv and MIP (Fig. 2, dots) issue from some cerebellar receiving thalamic territories (LIPv: CL and neighboring LP; MIP: VLc, VLps, CL, and LP) that relay inputs from the IP and D to the IPS (Kalil 1981; Asanuma et al. 1983; Stanton and Orr 1985; Amino et al. 2001). Major differences in thalamic input to LIPv and MIP (Fig. 2, dots) are in keeping with previous results (e.g., Schmahmann and Pandya 1990; Hardy and Lynch 1992; Amino et al. 2001) and are paralleled by topographical and functional differences in IP and D inputs to these areas, revealed in the present study (see below).

Cerebellar Nuclear Output Channels to LIPv

LIPv and LIPd form the "parietal eye field," which participates in saccade encoding (e.g., Colby and Goldberg 1999; Buneo and Andersen 2006). We found that LIPv receives prominent disynaptic cerebellar inputs from the caudal pole of D and from a restricted caudal portion of ventrolateral IP. Conversely,

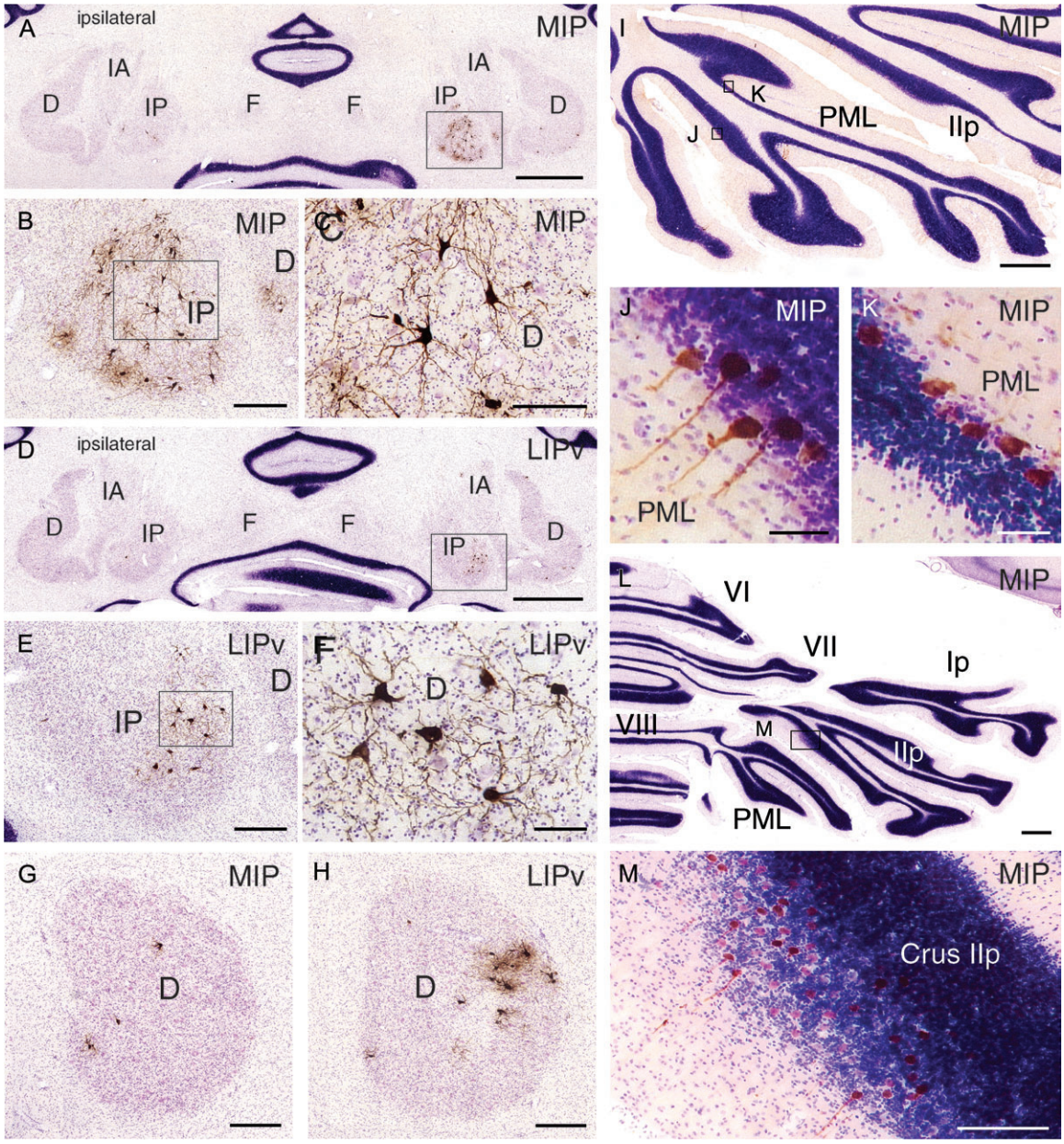

Figure 5. (*A–H*) Photomicrographs showing transneuronally labeled neurons in the cerebellar nuclei that target disynaptically the MIP and the LIPv, labeled at 2.5 days, and (*I–M*) cerebellar cortex PCs with trisynaptic inputs to MIP, labeled at 3 days. (*A–C*) MIP: labeling in ventrolateral IP and D (level shown in Fig. 3*D*); boxed area in (*A*) is enlarged in (*B*) (ventrolateral IP); high-power view in (*C*). (*D–F*) LIPv: labeling in ventrolateral IP and D (level shown in Fig. 3*D*). Boxed area in (*D*) is enlarged in (*E*) (ventrolateral IP); high-power view in (F). Note the more restricted distribution of labeled IP neurons that target LIPv (*E*) versus MIP (*B*). (*G, H*) Caudal pole of the D: at this level, D neurons targeting LIPv (*H*) are much more numerous than those targeting MIP (*G*), contrary to more rostral D levels (Figs 3, 4, and 6). (*I–K*) Distribution of labeled PC strips in PML, level shown in Fig. 7*d*, boxed areas in (*I*) are enlarged in (*J, K*). (*L, M*) Labeled PCs in Crus IIp (level shown in Fig. 7*b*). Boxed area in (*L*) is enlarged in (*M*). Scale bar = 2000 μm in (*A*) (also applies to *D*), 400 μm in (*B*) (also applies to *E, G, H, M*), 200 μm in (*C*), 100 μm in (*F*), 1000 μm in (*I*) (also applies to *L*), and 50 μm in (*J*) (also applies to *K*).

LIPd receives no cerebellar inputs (Clower et al. 2001). LIPd and LIPv differ in visual receptive field representation (Blatt et al. 1990; Ben Hamed et al. 2001) and connectivity. Notably, LIPv is the strongest source of LIP projections to the superior colliculus (SC) motor layers (Lynch et al. 1985) and frontal eye field (FEF) (Schall et al. 1995).

Caudal D Output Channels to LIPv

The caudal pole of the D, which targets LIPv (Fig. 3, right; Figs. 4, 5*H*, and 6), is especially responsive to teleceptive cues (Chapman et al. 1986; van Kan et al. 1993). It must be regarded as the D oculomotor domain because it also projects disynaptically to the FEF (Lynch et al. 1994) and monosynaptically to the SC (May et al. 1990), where it contacts directly saccade-related burst neurons (SRBNs) that target abducens motoneurons (Prevosto et al. 2007). Thus, the same caudal D domain influences in parallel LIPv, FEF, and SC SRBNs. This finding is important because these common targets of the caudal D have cooperative oculomotor functions and are heavily interconnected (Blatt et al. 1990; Colby and Goldberg 1999; Clower et al. 2001; Sommer and Wurtz 2008).

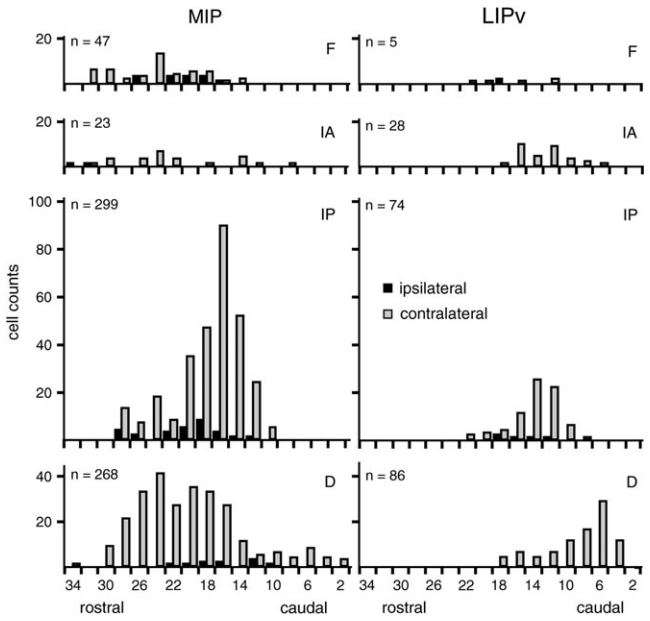

Figure 6. Histograms showing differences in number and rostrocaudal distribution of second-order neurons in the cerebellar nuclei (D, IP, IA, F) that target the MIP area and the LIPv area. Both areas receive major inputs from IP and D. Cell counts from 2 series of sections (spacing 200 μm). Black: ipsilateral; gray: contralateral. Sections are numbered (horizontal axis) from the caudal end of D. Total number of labeled cells is indicated on top of each histogram.

IP Output Channels to LIPv

The restricted caudal portion of the ventrolateral IP that targets LIPv (Fig. 3, right; Figs 4, 5*D–F*, and 6) is the distinct "eye movement" region (van Kan et al. 1993), related to vertical saccades and pursuit eye movements (Robinson et al. 1997; Robinson 2000; Robinson and Fuchs 2001). Unlike the caudal D, it does not provide output channels to FEF (Lynch et al. 1994). Although it heavily projects to the SC intermediate layers (May et al. 1990), its projections do not directly contact SRBNs (Prevosto et al. 2007), making it likely that they carry gaze (rather than purely saccade-related) signals to buildup, and eye/head neurons (Munoz and Wurtz 1995) and gaze dependent reach neurons in these SC layers (Lünenburger et al. 2001). Thus, it may transmit similar signals to LIPv. Notably, LIPv is prominently influenced by gaze position (Buneo and Andersen 2006) and is also involved in gaze saccades (Thier and Andersen 1998).

Cerebellar Nuclear Output Channels to MIP

The injected rostral MIP area functions as a sensorimotor interface for planning and control of proximal arm movements under visual and proprioceptive guidance (Mountcastle et al. 1975; Burbaud et al. 1991; Kalaska and Crammond 1992; Iriki et al. 1996; Johnson et al. 1996), like the parietal reach region (Buneo and Andersen 2006). Our results provide the first description of cerebellar nuclear and cortical populations potentially involved in the neuronal operations performed by MIP.

D Output Channels to MIP

MIP injections label neurons in the caudal two-thirds of the ventral D (especially its middle third) (Fig. 3, left; Figs 4 and 6). The results confirm that D projections to cortical areas are mediated by spatially separate output channels, by showing that the D population that targets MIP is entirely separate from D output channels to the supplementary motor area (SMA) (Wiesendanger and Wiesendanger 1985; Akkal et al. 2007) and arm M1 (Hoover and Strick 1999) and largely distinct from the D domains targeting AIP and 7b (Clower et al. 2001, 2005), LIPv (present results), dorsolateral prefrontal cortex (Middleton and Strick 2001), pre-SMA (Akkal et al. 2007), and ventral premotor cortex (PMv) (Orioli and Strick 1989).

IP Output Channels to MIP

IP output channels to MIP are prominently derived from the eye movement region that targets LIPv (see above) and from more medial, arm-related portions of the caudal ventrolateral IP (Mason et al. 1998) (Fig. 3, left; Figs 4, 5*A–C*, and 6). Some projections originate also from a more rostral portion of the ventrolateral IP (Fig. 3*B*) that is involved in divergence eye movements (Zhang and Gamlin 1998) and projects to the supraoculomotor area (May et al. 1992) and from there to abducens motoneurons (Ugolini, Klam, et al. 2006; Prevosto et al. 2007). Output channels to MIP from this divergence-related IP domain are consistent with the necessity of cooperative divergence during visually guided reaching (e.g., Melmoth and Grant 2006).

The strong projections to MIP from the caudal eye movement area of the ventrolateral IP may similarly reflect combined eye/arm movement coordination and might be involved in transmission of gaze signals (see above) contributing to the generation of nonretinocentric reference frames for eye–hand coordination. Notably, gaze influences on neuronal responses during reaching have been demonstrated in the SC (Lünenburger et al. 2001) and in PMv (Mushiake et al. 1997), which receive projections from this ventrolateral IP domain (SC: May et al. 1990; PMv: Orioli and Strick 1989). They have also been demonstrated in superior parietal lobe areas 5, 7m, PEc, and V6A (see Marzocchi et al. 2008) that are connected with MIP (e.g., Seltzer and Pandya 1986; Colby et al. 1988; Blatt et al. 1990; Shipp et al. 1998; Gamberini et al. 2009**;** Prevosto V, Graf W, and Ugolini G, unpublished results from the present experiments) and participate in multistage online control of reaching (e.g., Galletti et al. 2003; Battaglia-Mayer et al. 2006; Breveglieri et al. 2008).

By far, the most prominent output channels to MIP are derived from the arm-related portion of the ventrolateral IP (medial to the eye movement area), where neuronal activity is related to multijoint arm movements (reaching) (van Kan et al. 1993; Mason et al. 1998). The ventrolateral IP receives arm and neck proprioceptive signals directly from the external cuneate nucleus (Gonzalo-Ruiz and Leichnetz 1990), the rMAO (Ikeda et al. 1989), and the rostral spinocerebellar tract (Matsushita and Xiong 2001, rat). Notably, it can control reaching movements via its projections to the SC and underlying mesencephalic reticular formation (May et al. 1990) and to the arm/shoulder representation of the magnocellular red nucleus (Robinson et al. 1987), that is, descending motor pathways that mediate coordinated movements of the whole arm and, for the SC, also head movements and gaze (Keifer and Houk 1994; Belhaj-Saïf et al. 1998; Lünenburger et al. 2001). Output channels from the IP probably convey to MIP an efference copy of ongoing commands transmitted by the IP to tecto- and rubrospinal neurons because most interpositothalamic projections are axon collaterals of interpositotectal and interpositorubrospinal ones (Bentivoglio and Kuypers 1982; Keifer and Houk 1994).

Output channels to MIP from the ventrolateral IP may also be a potential substrate for adaptive modulation of visual–vestibular

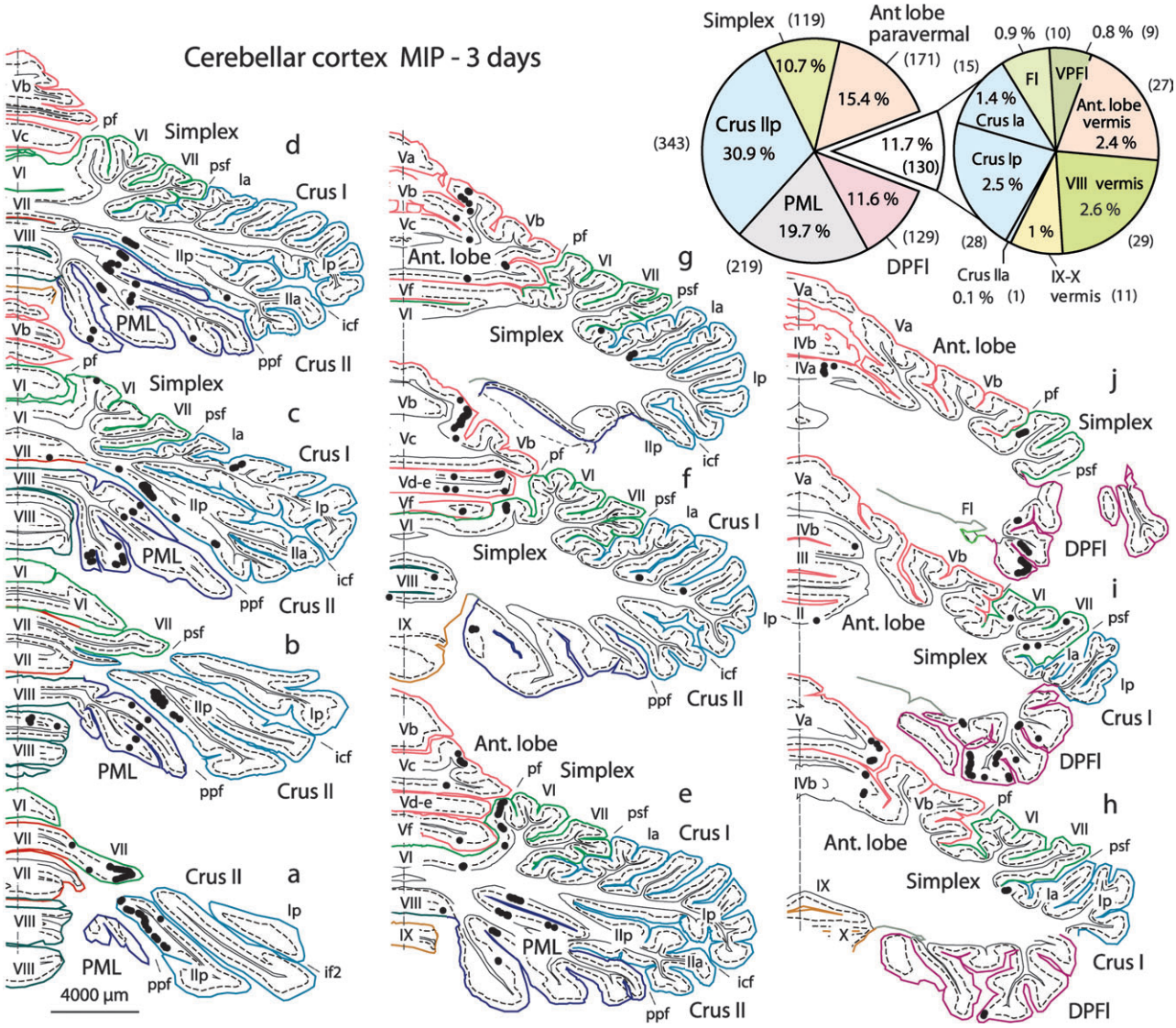

Figure 7. Right cerebellar cortex: distribution of PCs with trisynaptic inputs to the left MIP area, labeled transneuronally at 3 days with rabies virus. Cross-section levels (*a–j*): from caudal to rostral. Cerebellar lobules are named and color coded; fissures are named and indicated by a mark. Most labeled PCs are found in 3 main groups: obliquely oriented bands in the depth of Crus IIp and PML, multiple bands in DPFl, longitudinal bands in paravermal AL and simplex. Pie chart (top right): percentages and absolute numbers (in brackets) of labeled PCs in the different cerebellar subdivisions. Fl, flocculus; VPFl, ventral paraflocculus. Fissures (f): icf, intercrural f; if2, intracrural f 2; pf, primary f; ppf, prepyramidal f; psf, posterior superior f. See also Figures 5 and 8.

responses in MIP because IP neurons receive visual inputs from the NRTP (Gerrits and Voogd 1987) and DPFl (see below) and vestibular inputs (Luan and McCrea 2005) from the vestibular nuclei (Gonzalo-Ruiz and Leichnetz 1990) and the intermediate cerebellum (see below). Because distinct populations of interpositus neurons encode passive and active head movements (Luan and McCrea 2006), ventrolateral IP output channels to MIP (and PMv) may contribute to known differences in neuronal responses to active and passive head movements in MIP (Klam and Graf 2006) and PMv (Graziano et al. 1997). The rostral F may also participate to these properties (e.g., Meng et al. 2007), although it has only minor projections to MIP (Figs 4 and 6).

PCs Inputs to MIP

Cerebellar PC strips that influence MIP trisynaptically via their projections to the ventrolateral IP and ventral D originate predominantly (61.2%) from the posterior cerebellum (50.6% in PML/Crus IIp, 11.6% in DPFl) (Figs 7 and 8), in striking contrast with PCs output channels to arm M1, which are derived mostly (80%) from the anterior cerebellum (AL/simplex) (Kelly and Strick 2003; Lu et al. 2007). Moreover, in the anterior cerebellum, PC populations targeting MIP (present study) and M1 (Kelly and Strick 2003; Lu et al. 2007) are remarkably separate, a segregation also present in the respective D and interpositus populations (M1: Hoover and Strick 1999; Lu et al. 2007). Thus, PCs targeting MIP form sparse longitudinal strips, largely in paravermal portions of lobules V/VI of AL/simplex (Figs 7 and 8). In contrast, PCs targeting arm M1 are located more laterally (Kelly and Strick 2003; Lu et al. 2007).

A distinctive characteristic of the posterior cerebellar cortical areas (DPFl, PML/Crus IIp) that provide prominent output channels to MIP (62,2% of the total, present study), and also M1

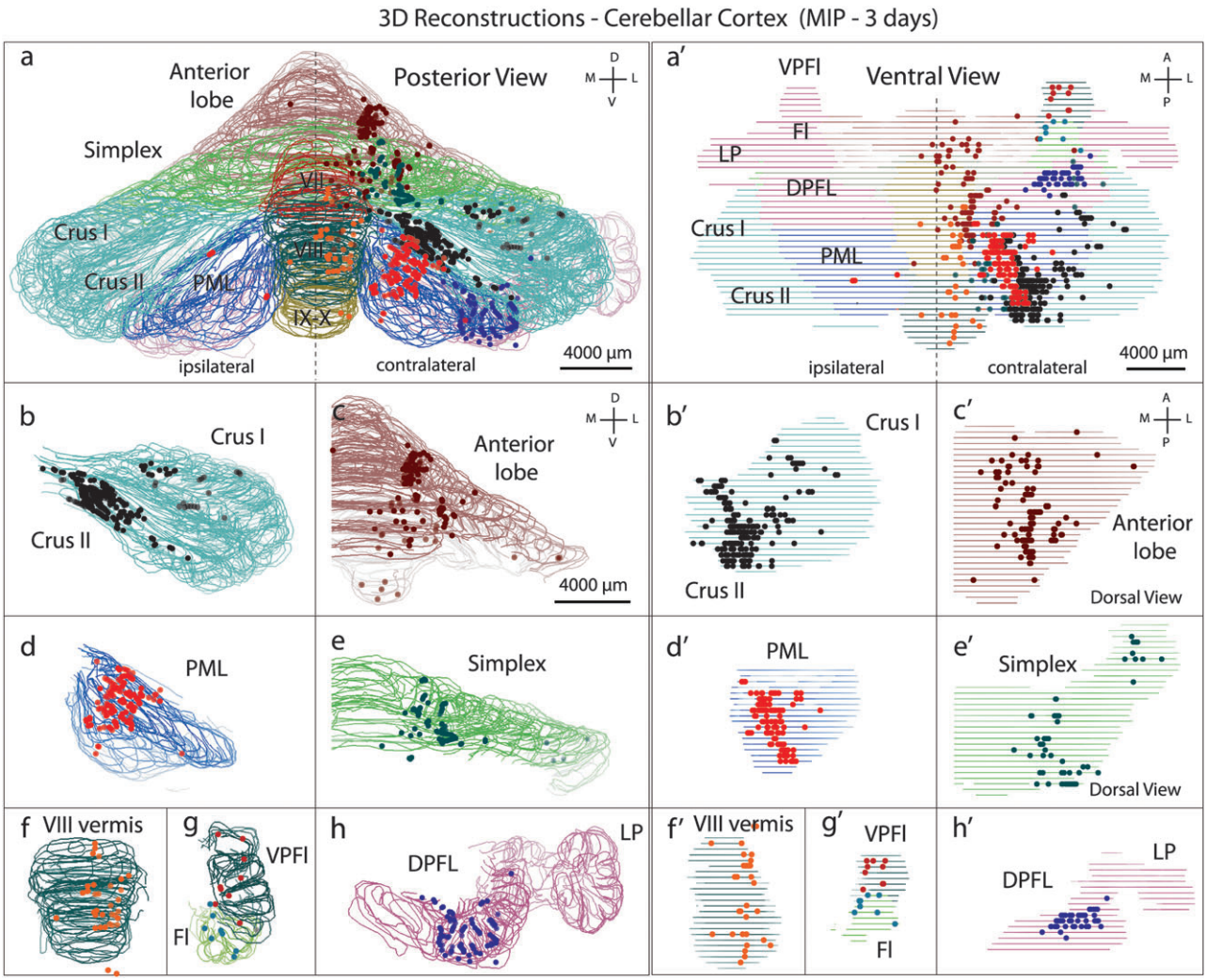

Figure 8. 3D reconstruction of the cerebellar cortex, showing the organization of PCs providing trisynaptic inputs to MIP (3 days). 3D reconstructions were made using Neurolucida. Posterior views (left) and ventral views (right) are shown here in wireframe mode for the entire cerebellar cortex (*a, a′*) and for individual divisions on the right (framed images *b–h* and *b′–h′*). Cerebellar divisions are color coded as in Figure 7 (cross sections). Most labeled PCs are found in Crus IIp and PML, DPFl, and paravermal AL and simplex. Other abbreviations: D, dorsal; Fl, flocculus; M, medial; L, lateral; LP, lobus petrosus; V, ventral; VPFl, ventral paraflocculus.

(20%, Kelly and Strick 2003), is that they have the required connectivity for visual guidance of reaching. In fact, they receive projections from the dorsolateral pons, relaying elaborate visual spatial representations from parietal dorsal stream areas, including MIP, as well as visuomotor inputs from the SC (Glickstein et al. 1994). Moreover, they are the cerebellar areas showing the most pronounced activations during visually guided reaching tasks (Savaki et al. 1996) and receive the central and peripheral inputs that are required for comparison between intended and actual arm movements (see below).

Dorsal Paraflocculus

Notably, the DPFl projects exclusively to the ventral D and ventrolateral IP (Kralj-Hans et al. 2007), which target MIP (see above). It receives the greatest number of projections from the dorsolateral pons (Stein and Glickstein 1992; Glickstein et al. 1994) and has prominent visual and eye movement–related activity (Noda and Mikami 1986; Marple-Horvat and Stein 1990). Its properties are much more tightly related to visual guidance than movement execution (Stein and Glickstein 1992), as it lacks the motor cortical and arm proprioceptive inputs that reach the PML/Crus IIp (see below) and shows only limited arm movement–related activity (Marple-Horvat and Stein 1985, 1987, 1990).

Paramedian Lobule and Crus II Posterior

The portions of PML/Crus IIp that influence MIP (Figs 7 and 8) belong to the arm representation of the posterior cerebellum (Snider and Eldred 1952) and have activity related to arm movements (Marple-Horvat and Stein 1987). The labeled portions of PML/Crus IIp may be regarded as a functional unit because they largely receive common inputs and have the required connectivity to code for incoming forelimb movement parameters, by combining motor plans with reafferent proprioceptive inputs. In fact, they receive mossy and climbing fiber inputs from motor areas, premotor areas, frontal association, and parietal cortex, including area 5 (e.g., Sasaki et al. 1977; Brodal 1980; Kelly and Strick 2003) and prominent extero- and

proprioceptive inputs from the arm through olivo-, cuneo-, and rostral spinocerebellar pathways (e.g., Rosina and Provini 1983; Jasmin and Courville 1987; Matsushita and Ikeda 1987). They also receive vestibular and neck inputs related to head movements from the central cervical nucleus (Matsushita and Tanami 1987), direct projections from the vestibular nuclei (Jasmin and Courville 1987), and eye position signals from the nucleus prepositus hypoglossi (Brodal and Brodal 1983). This conjunction of inputs is consistent with the role of PML/Crus IIp PC strips in visual and proprioceptive guidance of reaching, and possibly coordination of arm/eye/head movement (Stein and Glickstein 1992; Desmurget and Grafton 2000; Miall et al. 2001).

Functional Considerations

Forward Models of Action and Optic Ataxia

How mechanisms for adaptive and online control of movement are implemented in the brain is highly disputed. The cerebellum and the PPC are suggested to produce forward models of action required for online control of movement (Desmurget and Grafton 2000; Buneo and Andersen 2006). The cerebellar cortical and nuclear output channels to MIP, demonstrated here, potentially form a suitable neural substrate for predictive control of voluntary action and online control mechanisms, allowing for fast correction of movement execution based on an efference copy of motor signals and visual and proprioceptive feedback (Blakemore and Sirigu 2003). Notably, lesions of the superior parietal lobe, or restricted to the medial bank of the IPS (Trillenberg et al. 2007), result in optic ataxia, a deficit in reaching movements under visual as well as proprioceptive guidance (Blangero et al. 2007). Considering the role of the cerebellar cortical and nuclear pathways to MIP in visual and proprioceptive guidance of movement, their disruption may contribute to the specific deficits in online control of movement associated with optic ataxia (e.g., Pisella et al. 2000; Trillenberg et al. 2007).

Adaptive Visuospatial Signals and Prism Adaptation

Another unresolved issue is the respective involvement and connectivity of the cerebellum and PPC in prism adaptation, which is particularly effective and long lasting in alleviating visuospatial (extrapersonal) neglect symptoms following parietal lesions (Frassinetti et al. 2002; Redding and Wallace 2006). Our results reveal one of the potential neural bases for such prism adaptation effects, by demonstrating that MIP receives major projections, via the ventral D and ventrolateral IP, from posterior cerebellar cortical regions (DFPl, PML/Crus IIp) that have been proposed to mediate prism adaptation (Baizer et al. 1999). Notably, these cerebellar projections to MIP could mediate prism-induced recalibration mechanisms in neglect patients because they remain functional, since the superior parietal lobe and IPS are not typically part of the cortical lesions leading to neglect (Milner and McIntosh 2005; Striemer et al. 2008). Conversely, lesions of the medial bank of the IPS that cause optic ataxia (Trillenberg et al. 2007) also disrupt the beneficial effects of prism adaptation on neglect symptoms (Striemer et al. 2008), and both effects might be explained by the impairment of the cerebellar inputs to the IPS demonstrated by the present study. The finding that the same ventrolateral IP domain targets both the IPS and PMv, that is implicated in prism adaptation effects (Kurata and Hoshi 1999), points to this IP domain as the critical cerebellar output channel involved in transmission to the cerebral cortex of adaptive signals that serve to redirect visuospatial attention (i.e., the beneficial effects of prism adaptation on extrapersonal neglect) and may similarly contribute to online updating of extrapersonal space representations in the IPS and PMv (e.g., Graziano and Gross 1998; Maravita and Iriki 2004).

Funding

European Union EU 5th Framework Programme (QLRT-2001-00151, EUROKINESIS); Specialized Neuroscience Research Program (SNRP): NIH/NINDS U54 NS-39407 and NSF-PIRE (0730255).

Notes

We thank Bénédicte Leveillé, Marie-Annick Thomas, and Suzette Doutremer for technical assistance. *Conflict of Interest*: None declared.

Address correspondence to Dr Gabriella Ugolini, Laboratoire de Neurobiologie Cellulaire et Moléculaire (NBCM), UPR9040, Bât 32 CNRS, 1 av de la Terrasse, 91198 Gif sur Yvette, France. Email: gabriella.ugolini@nbcm.cnrs-gif.fr

References

Akkal D, Dum RP, Strick PL. 2007. Supplementary motor area and presupplementary motor area: targets of basal ganglia and cerebellar output. J Neurosci. 27:10659–10673.

Amino Y, Kyuhou S, Matsuzaki R, Gemba H. 2001. Cerebello-thalamocortical projections to the posterior parietal cortex in the macaque monkey. Neurosci Lett. 309:29–32.

Asanuma C, Andersen RA, Cowan WM. 1985. The thalamic relations of the caudal inferior parietal lobule and the lateral prefrontal cortex in monkeys: divergent cortical projections from cell clusters in the medial pulvinar nucleus. J Comp Neurol. 241:357–381.

Asanuma C, Thach WR, Jones EG. 1983. Anatomical evidence for segregated focal groupings of efferent cells and their terminal ramifications in the cerebellothalamic pathway of the monkey. Brain Res. 286:267–297.

Baizer JS, Kralj-Hans I, Glickstein M. 1999. Cerebellar lesions and prism adaptation in macaque monkeys. J Neurophysiol. 81:1960–1965.

Battaglia-Mayer A, Archambault PS, Caminiti R. 2006. The cortical network for eye-hand coordination and its relevance to understanding motor disorders of parietal patients. Neuropsychologia. 44:2607–2620.

Belhaj-Saïf A, Karrer JH, Cheney PD. 1998. Distribution and characteristics of poststimulus effects in proximal and distal forelimb muscles from red nucleus in the monkey. J Neurophysiol. 79:1777–1789.

Ben Hamed S, Duhamel JR, Bremmer F, Graf W. 2001. Representation of the visual field in the lateral intraparietal area of macaque monkeys: a quantitative receptive field analysis. Exp Brain Res. 140:127–144.

Bentivoglio M, Kuypers HGJM. 1982. Divergent axon collaterals from rat cerebellar nuclei to diencephalon, mesencephalon, medulla oblongata and cervical cord–a fluorescent double retrograde labeling study. Exp Brain Res. 46:339–356.

Billig I, Strick PL. 2006. Can one mix cholera toxin with rabies virus in tracing experiments? Program No. 694.2/PP82, Abstract Viewer/Itinerary Planner, 2006 October 14–18; Atlanta (GA): Society for Neuroscience. Online.

Bioulac B, Seal J, Guehl D, Burbaud P, Gross C. 1999. Reorganization of area 5 neuron activity in trained deafferented monkeys. Brain Res. 835:266–274.

Blakemore SJ, Sirigu A. 2003. Action prediction in the cerebellum and in the parietal lobe. Exp Brain Res. 153:239–245.

Blangero A, Ota H, Delporte L, Revol P, Vindras P, Rode G, Boisson D, Vighetto A, Rossetti Y, Pisella L. 2007. Optic ataxia is not only 'optic': impaired spatial integration of proprioceptive information. NeuroImage. 36(Suppl 2):T61–T68.

Blatt GJ, Andersen RA, Stoner GR. 1990. Visual receptive field organization and cortico-cortical connections of the lateral intraparietal area (area LIP) in the macaque. J Comp Neurol. 299:421–445.

Bremmer F, Klam F, Duhamel JR, Ben Hamed S, Graf W. 2002. Visual-vestibular interactive responses in the macaque ventral intraparietal area (VIP). Eur J Neurosci. 16:1569–1586.
Breveglieri R, Galletti C, Monaco S, Fattori P. 2008. Visual, somatosensory, and bimodal activities in the macaque parietal area PEc. Cereb Cortex. 18:806–816.
Brodal A, Brodal P. 1983. Observations on the projection from the perihypoglossal nuclei onto the cerebellum in the macaque monkey. Arch Ital Biol. 121:151–166.
Brodal P. 1980. The projection from the nucleus reticularis tegmenti pontis to the cerebellum in the rhesus monkey. Exp Brain Res. 38:29–36.
Buneo CA, Andersen RA. 2006. The posterior parietal cortex: sensorimotor interface for the planning and online control of visually guided movements. Neuropsychologia. 44:2594–2606.
Burbaud P, Doegle C, Gross C, Bioulac B. 1991. A quantitative study of neuronal discharge in areas 5, 2, and 4 of the monkey during fast arm movements. J Neurophysiol. 66:429–443.
Chapman CE, Spidalieri G, Lamarre Y. 1986. Activity of dentate neurons during arm movements triggered by visual, auditory, and somesthetic stimuli in the monkey. J Neurophysiol. 55:203–226.
Clower DM, Dum RP, Strick PL. 2005. Basal ganglia and cerebellar inputs to 'AIP'. Cereb Cortex. 15:913–920.
Clower DM, West RA, Lynch JC, Strick PL. 2001. The inferior parietal lobule is the target of output from the superior colliculus, hippocampus, and cerebellum. J Neurosci. 21:6283–6291.
Colby CL, Duhamel JR. 1991. Heterogeneity of extrastriate visual areas and multiple parietal areas in the macaque monkey. Neuropsychologia. 29:517–537.
Colby CL, Gattass R, Olson CR, Gross CG. 1988. Topographical organization of cortical afferents to extrastriate visual area PO in the macaque: a dual tracer study. J Comp Neurol. 269:392–413.
Colby CL, Goldberg ME. 1999. Space and attention in parietal cortex. Annu Rev Neurosci. 22:319–349.
Crammond DJ, Kalaska JF. 1989. Neuronal activity in primate parietal cortex area 5 varies with intended movement direction during an instructed-delay period. Exp Brain Res. 76:458–462.
Desmurget M, Grafton S. 2000. Forward modeling allows feedback control for fast reaching movements. Trends Cogn Sci. 4:423–431.
Dum RP, Strick PL. 2003. An unfolded map of the cerebellar dentate nucleus and its projections to the cerebral cortex. J Neurophysiol. 89:634–639.
Frassinetti F, Angeli V, Meneghello F, Avanzi S, Ladavas E. 2002. Long-lasting amelioration of visuospatial neglect by prism adaptation. Brain. 125:608–623.
Galletti C, Kutz DF, Gamberini M, Breveglieri R, Fattori P. 2003. Role of the medial parieto-occipital cortex in the control of reaching and grasping movements. Exp Brain Res. 153:158–170.
Gamberini M, Passarelli L, Fattori P, Zucchelli M, Bakola S, Luppino G, Galletti C. 2009. Cortical connections of the visuomotor parietooccipital area V6Ad of the macaque monkey. J Comp Neurol. 513:622–642.
Gerrits NM, Voogd J. 1987. The projection of the nucleus reticularis tegmenti pontis and adjacent regions of the pontine nuclei to the central cerebellar nuclei in the cat. J Comp Neurol. 258:52–69.
Glickstein M, Gerrits N, Kralj-Hans I, Mercier B, Stein J, Voogd J. 1994. Visual pontocerebellar projections in the macaque. J Comp Neurol. 349:1–72.
Gonzalo-Ruiz A, Leichnetz GR. 1990. Connections of the caudal cerebellar interpositus complex in a new world monkey (Cebus apella). Brain Res Bull. 25:919–927.
Graf W, Prevosto V, Ugolini G. 2006. Differences in disynaptic fronto-parietal input from arcuate and premotor cortex to medial (MIP/VIPm) and lateral (VIPl/LIPv) intraparietal areas, revealed by retrograde transneuronal transfer of rabies virus. Program No. 242.17. Abstract Viewer/Itinerary Planner, 2006 October 14–18; Atlanta (GA): Society for Neuroscience. Online.
Graziano MS, Gross CG. 1998. Spatial maps for the control of movement. Curr Opin Neurobiol. 8:195–201.
Graziano MS, Hu XT, Gross CG. 1997. Visuospatial properties of ventral premotor cortex. J Neurophysiol. 77:2268–2292.
Hamel-Pâquet C, Sergio LE, Kalaska JF. 2006. Parietal area 5 activity does not reflect the differential time-course of motor output kinetics during arm-reaching and isometric-force tasks. J Neurophysiol. 95:3353–3370.
Hardy SG, Lynch JC. 1992. The spatial distribution of pulvinar neurons that project to two subregions of the inferior parietal lobule in the macaque. Cereb Cortex. 2:217–230.
Hoover JE, Strick PL. 1999. The organization of cerebellar and basal ganglia outputs to primary motor cortex as revealed by retrograde transneuronal transport of herpes simplex virus type 1. J Neurosci. 19:1446–1463.
Ikeda Y, Noda H, Sugita S. 1989. Olivocerebellar and cerebelloolivary connections of the oculomotor region of the fastigial nucleus in the macaque monkey. J Comp Neurol. 284:463–488.
Iriki A, Tanaka M, Iwamura Y. 1996. Coding of modified body schema during tool use by macaque postcentral neurones. Neuroreport. 7:2325–2330.
Jasmin L, Courville J. 1987. Distribution of external cuneate nucleus afferents to the cerebellum: I. Notes on the projections from the main cuneate and other adjacent nuclei. An experimental study with radioactive tracers in the cat. J Comp Neurol. 261:481–496.
Johnson PB, Ferraina S, Bianchi L, Caminiti R. 1996. Cortical networks for visual reaching: physiological and anatomical organization of frontal and parietal lobe arm regions. Cereb Cortex. 6:102–119.
Kakei S, Yagi J, Wannier T, Na J, Shinoda Y. 1995. Cerebellar and cerebral inputs to corticocortical and corticofugal neurons in areas 5 and 7 in the cat. J Neurophysiol. 74:400–412.
Kalaska JF, Crammond DJ. 1992. Cerebral cortical mechanisms of reaching movements. Science. 255:1517–1523.
Kalil K. 1981. Projections of the cerebellar and dorsal column nuclei upon the thalamus of the rhesus monkey. J Comp Neurol. 195: 25–50.
Keifer J, Houk JC. 1994. Motor function of the cerebellorubrospinal system. Physiol Rev. 74:509–542.
Kelly RM, Strick PL. 2003. Cerebellar loops with motor cortex and prefrontal cortex of a nonhuman primate. J Neurosci. 23: 8432–8444.
Klam F, Graf W. 2003. Vestibular response kinematics in posterior parietal cortex neurons of macaque monkeys. Eur J Neurosci. 18:995–1010.
Klam F, Graf W. 2006. Discrimination between active and passive head movements by macaque ventral and medial intraparietal cortex neurons. J Physiol. 574:367–386.
Kralj-Hans I, Baizer JS, Swales C, Glickstein M. 2007. Independent roles for the dorsal paraflocculus and vermal lobule VII of the cerebellum in visuomotor coordination. Exp Brain Res. 177:209–222.
Kurata K, Hoshi E. 1999. Reacquisition deficits in prism adaptation after muscimol microinjection into the ventral premotor cortex of monkeys. J Neurophysiol. 81:1927–1938.
Lewis JW, Van Essen DC. 2000. Mapping of architectonic subdivisions in the macaque monkey, with emphasis on parieto-occipital cortex. J Comp Neurol. 428:79–111.
Lu X, Miyachi S, Ito Y, Nambu A, Takada M. 2007. Topographic distribution of output neurons in cerebellar nuclei and cortex to somatotopic map of primary motor cortex. Eur J Neurosci. 25:2374–2382.
Luan H, McCrea R. 2005. Convergence of vestibular and proprioceptive signals on cerebellar nucleus thalamus projection neurons in the squirrel monkey Program No. 392.5 Abstract Viewer/Itinerary Planner Conference, 2005 November 12–16; Washington (DC): Society for Neuroscience.
Luan H, McCrea R. 2006. Interactions of vestibular, neck proprioceptive head movement motor signals in the cerebellar interpositus nucleus. Program No. 139.11/D76 Neuroscience Meeting Planner Conference, 2006 October 14–18; Atlanta (GA): Society for Neuroscience.
Lünenburger L, Kleiser R, Stuphorn V, Miller LE, Hoffmann KP. 2001. A possible role of the superior colliculus in eye-hand coordination. Prog Brain Res. 134:109–125.
Luppi PH, Fort P, Jouvet M. 1990. Iontophoretic application of unconjugated cholera toxin B subunit (CTb) combined with

immunohistochemistry of neurochemical substances: a method for transmitter identification of retrogradely labeled neurons. Brain Res. 534:209–224.
Lynch JC, Graybiel AM, Lobeck LJ. 1985. The differential projection of two cytoarchitectonic subregions of the inferior parietal lobule of macaque upon the deep layers of the superior colliculus. J Comp Neurol. 235:241–254.
Lynch JC, Hoover JE, Strick PL. 1994. Input to the primate frontal eye field from the substantia nigra, superior colliculus, and dentate nucleus demonstrated by transneuronal transport. Exp Brain Res. 100:181–186.
Madigan JC, Jr, Carpenter MB. 1971. Cerebellum of the rhesus monkey: atlas of lobules, laminae, and folia in sections. Baltimore (MD): University Park Press.
Maravita A, Iriki A. 2004. Tools for the body (schema). Trends Cogn Sci. 8:79–86.
Marple-Horvat DE, Stein JF. 1985. Role of different cerebellar regions in visuomotor control. Neurosci Lett. (Suppl 21):S11.
Marple-Horvat DE, Stein JF. 1987. Cerebellar neuronal activity related to arm movements in trained rhesus monkeys. J Physiol. 394: 351–366.
Marple-Horvat DE, Stein JF. 1990. Neuronal activity in the lateral cerebellum of trained monkeys, related to visual stimuli or to eye movements. J Physiol. 428:595–614.
Marzocchi N, Breveglieri R, Galletti C, Fattori P. 2008. Reaching activity in parietal area V6A of macaque: eye influence on arm activity or retinocentric coding of reaching movements? Eur J Neurosci. 27:775–789.
Mason CR, Miller LE, Baker JF, Houk JC. 1998. Organization of reaching and grasping movements in the primate cerebellar nuclei as revealed by focal muscimol inactivations. J Neurophysiol. 79:537–554.
Matelli M, Govoni P, Galletti C, Kutz DF, Luppino G. 1998. Superior area 6 afferents from the superior parietal lobule in the macaque monkey. J Comp Neurol. 402:327–352.
Matsushita M, Ikeda M. 1987. Spinocerebellar projections from the cervical enlargement in the cat, as studied by anterograde transport of wheat germ agglutinin-horseradish peroxidase. J Comp Neurol. 263:223–240.
Matsushita M, Tanami T. 1987. Spinocerebellar projections from the central cervical nucleus in the cat, as studied by anterograde transport of wheat germ agglutinin-horseradish peroxidase. J Comp Neurol. 266:376–397.
Matsushita M, Xiong G. 2001. Uncrossed and crossed projections from the upper cervical spinal cord to the cerebellar nuclei in the rat, studied by anterograde axonal tracing. J Comp Neurol. 432:101–118.
May PJ, Hartwich-Young R, Nelson J, Sparks DL, Porter JD. 1990. Cerebellotectal pathways in the macaque: implications for collicular generation of saccades. Neuroscience. 36:305–324.
May PJ, Porter JD, Gamlin PD. 1992. Interconnections between the primate cerebellum and midbrain near-response regions. J Comp Neurol. 315:98–116.
Melmoth DR, Grant S. 2006. Advantages of binocular vision for the control of reaching and grasping. Exp Brain Res. 171:371–388.
Meng H, May PJ, Dickman JD, Angelaki DE. 2007. Vestibular signals in primate thalamus: properties and origins. J Neurosci. 27:13590–13602.
Miall RC, Reckess GZ, Imamizu H. 2001. The cerebellum coordinates eye and hand tracking movements. Nat Neurosci. 4:638–644.
Middleton FA, Strick PL. 2001. Cerebellar projections to the prefrontal cortex of the primate. J Neurosci. 21:700–712.
Milner AD, McIntosh RD. 2005. The neurological basis of visual neglect. Curr Opin Neurol. 18:748–753.
Moschovakis AK, Gregoriou GG, Ugolini G, Doldan M, Graf W, Guldin W, Hadjidimitrakis K, Savaki HE. 2004. Oculomotor areas of the primate frontal lobes: a transneuronal transfer of rabies virus and 14C -2-deoxyglucose functional imaging study. J Neurosci. 24:5726–5740.
Mountcastle VB, Lynch JC, Georgopoulos A, Sakata H, Acuna C. 1975. Posterior parietal association cortex of the monkey: command functions for operations within extrapersonal space. J Neurophysiol. 38:871–908.
Mulliken GH, Musallam S, Andersen RA. 2008. Forward estimation of movement state in posterior parietal cortex. Proc Natl Acad Sci U S A. 105:8170–8177.
Munoz DP, Wurtz RH. 1995. Saccade-related activity in monkey superior colliculus. I. Characteristics of burst and buildup cells. J Neurophysiol. 73:2313–2333.
Mushiake H, Tanatsugu Y, Tanji J. 1997. Neuronal activity in the ventral part of premotor cortex during target-reach movement is modulated by direction of gaze. J Neurophysiol. 78:567–571.
Noda H, Mikami A. 1986. Discharges of neurons in the dorsal paraflocculus of monkeys during eye movements and visual stimulation. J Neurophysiol. 56:1129–1146.
Olszewski J. 1952. The thalamus of the Macaca mulatta, an atlas for use with the stereotaxic instrument. Basel (NY): S. Karger.
Orioli PJ, Strick PL. 1989. Cerebellar connections with the motor cortex and the arcuate premotor area: an analysis employing retrograde transneuronal transport of WGA-HRP. J Comp Neurol. 288:612–626.
Pisella L, Grea H, Tilikete C, Vighetto A, Desmurget M, Rode G, Boisson D, Rossetti Y. 2000. An 'automatic pilot' for the hand in human posterior parietal cortex: toward reinterpreting optic ataxia. Nat Neurosci. 3:729–736.
Prevosto V, Ugolini G, Graf W. 2007. Cerebellar control of eye movements: polysynaptic inputs from fastigial, interpositus posterior and dentate nuclei to lateral rectus motoneurons in primates, revealed by retrograde transneuronal transfer of rabies virus. Program No. 718.10. Abstract Viewer/Itinerary Planner, 2007 November 3–7; San Diego (CA): Society for Neuroscience Online.
Redding GM, Wallace B. 2006. Prism adaptation and unilateral neglect: review and analysis. Neuropsychologia. 44:1–20.
Robinson FR. 2000. Role of the cerebellar posterior interpositus nucleus in saccades. I. Effect of temporary lesions. J Neurophysiol. 84:1289–1302.
Robinson FR, Fuchs AF. 2001. The role of the cerebellum in voluntary eye movements. Annu Rev Neurosci. 24:981–1004.
Robinson FR, Houk JC, Gibson AR. 1987. Limb specific connections of the cat magnocellular red nucleus. J Comp Neurol. 257:553–577.
Robinson FR, Straube A, Fuchs AF. 1997. Participation of caudal fastigial nucleus in smooth pursuit eye movements II Effects of muscimol inactivation. J Neurophysiol. 78:848–859.
Rosina A, Provini L. 1983. Somatotopy of climbing fiber branching to the cerebellar cortex in cat. Brain Res. 289:45–63.
Sasaki K, Oka H, Kawaguchi S, Jinnai K, Yasuda T. 1977. Mossy fibre and climbing fibre responses produced in the cerebeller cortex by stimulation of the cerebral cortex in monkeys. Exp Brain Res. 29:419–428.
Savaki HE, Kennedy C, Sokoloff L, Mishkin M. 1996. Visually guided reaching with the forelimb contralateral to a "blind" hemisphere in the monkey: contribution of the cerebellum. Neuroscience. 75: 143–159.
Schall JD, Morel A, King DJ, Bullier J. 1995. Topography of visual cortex connections with frontal eye field in macaque: convergence and segregation of processing streams. J Neurosci. 15:4464–4487.
Schmahmann JD, Pandya DN. 1990. Anatomical investigation of projections from thalamus to posterior parietal cortex in the rhesus monkey: a WGA-HRP and fluorescent tracer study. J Comp Neurol. 295:299–326.
Schmued LC. 1990. A rapid, sensitive histochemical stain for myelin in frozen brain sections. J Histochem Cytochem. 38:717–720.
Seal J, Gross C, Bioulac B. 1982. Activity of neurons in area 5 during a simple arm movement in monkeys before and after deafferentation of the trained limb. Brain Res. 250:229–243.
Seltzer B, Pandya DN. 1986. Posterior parietal projections to the intraparietal sulcus of the rhesus monkey. Exp Brain Res. 62:459–469.
Shipp S, Blanton M, Zeki S. 1998. A visuo-somatomotor pathway through superior parietal cortex in the macaque monkey: cortical connections of areas V6 and V6A. Eur J Neurosci. 10:3171–3193.
Snider RS, Eldred E. 1952. Cerebrocerebellar relationships in the monkey. J Neurophysiol. 15:27–40.
Sommer MA, Wurtz RH. 2008. Brain circuits for the internal monitoring of movements. Annu Rev Neurosci. 31:317–38.

Stanton GB, Orr A. 1985. [3H]Choline labeling of cerebellothalamic neurons with observations on the cerebello-thalamo-parietal pathway in cats. Brain Res. 335:237–243.
Stein JF, Glickstein M. 1992. Role of the cerebellum in visual guidance of movement. Physiol Rev. 72:967–1017.
Striemer C, Blangero A, Rossetti Y, Boisson D, Rode G, Salemme R, Vighetto A, Pisella L, Danckert J. 2008. Bilateral parietal lesions disrupt the beneficial effects of prism adaptation: evidence from a patient with optic ataxia. Exp Brain Res. 187:295–302.
Thier P, Andersen RA. 1998. Electrical microstimulation distinguishes distinct saccade-related areas in the posterior parietal cortex. J Neurophysiol. 80:1713–1735.
Trillenberg P, Sprenger A, Petersen D, Kompf D, Heide W, Helmchen C. 2007. Functional dissociation of saccade and hand reaching control with bilateral lesions of the medial wall of the intraparietal sulcus: implications for optic ataxia. Neuroimage. 36(Suppl 2):T69–T76.
Ugolini G. 1995. Specificity of rabies virus as a transneuronal tracer of motor networks: transfer from hypoglossal motoneurons to connected second-order and higher order central nervous system cell groups. J Comp Neurol. 356:457–480.
Ugolini G. 2008. Use of rabies virus as a transneuronal tracer of neuronal connections: implications for the understanding of rabies pathogenesis. Dev Biol (Basel). 131:493–506.
Ugolini G, Klam F, Doldan Dans M, Dubayle D, Brandi AM, Büttner-Ennever J, Graf W. 2006. Horizontal eye movement networks in primates as revealed by retrograde transneuronal transfer of rabies virus: differences in monosynaptic input to "slow" and "fast" abducens motoneurons. J Comp Neurol. 498:762–785.
Ugolini G, Klam F, Prevosto V, Graf W. 2005. Cerebellar nuclear input to posterior parietal areas VIP/MIP, revealed by retrograde transneuronal transfer of rabies virus. Program No. 289.7. Abstract Viewer/Itinerary Planner, 2005 November 12–16; Washington (DC): Society for Neuroscience Online.
Ugolini G, Prevosto V, Graf W. 2006. Differences in cerebellar nuclear input to medial (MIP/VIPm) and lateral (VIPl/LIPv) intraparietal areas, revealed by retrograde transneuronal transfer of rabies virus. Program No. 242.19. Abstract Viewer/Itinerary Planner, 2006 October 14–18; Atlanta (GA): Society for Neuroscience Online.
Ugolini G, Prevosto V, Graf W. 2007. Cerebellar cortical and nuclear output channels to the medial intraparietal area (MIP): pathways for online and adaptive control of proprioceptive and visual guidance of reaching, revealed by retrograde transneuronal transfer of rabies virus. Program No. 618.21. Abstract Viewer/Itinerary Planner, 2007 November 3–7; San Diego (CA): Society for Neuroscience Online.
van Kan PL, Houk JC, Gibson AR. 1993. Output organization of intermediate cerebellum of the monkey. J Neurophysiol. 69: 57–73.
Voogd J, Pardoe J, Ruigrok TJ, Apps R. 2003. The distribution of climbing and mossy fiber collateral branches from the copula pyramidis and the paramedian lobule: congruence of climbing fiber cortical zones and the pattern of zebrin banding within the rat cerebellum. J Neurosci. 23:4645–4656.
Wiesendanger R, Wiesendanger M. 1985. Cerebello-cortical linkage in the monkey as revealed by transcellular labeling with the lectin wheat germ agglutinin conjugated to the marker horseradish peroxidase. Exp Brain Res. 59:105–117.
Zhang H, Gamlin PD. 1998. Neurons in the posterior interposed nucleus of the cerebellum related to vergence and accommodation I Steady-state characteristics. J Neurophysiol. 79:1255–1269.